Polymer 49 (2008) 4846–4851

Contents lists available at ScienceDirect

Polymer

journal homepage: www.elsevier.com/locate/polymer

# Conductivity enhancement of carbon nanotube and nanofiber-based polymer nanocomposites by melt annealing

Bani H. Cipriano [a], Arun K. Kota [b], Alan L. Gershon [b], Conrad J. Laskowski [b], Takashi Kashiwagi [c], Hugh A. Bruck [b,*], Srinivasa R. Raghavan [a,**]

[a] Departments of Chemical and Biomolecular Engineering, University of Maryland, College Park, MD 20742-2111, United States
[b] Department of Mechanical Engineering, University of Maryland, College Park, MD 20742-2111, United States
[c] Fire Research Division, Building and Fire Research Laboratory, National Institute of Standards and Technology, Gaithersburg, MD 20878, United States

ARTICLE INFO

*Article history:*
Received 8 June 2008
Accepted 24 August 2008
Available online 13 September 2008

*Keywords:*
Polystyrene
Melt annealing
Nanocomposite

ABSTRACT

The addition of multi-walled carbon nanotubes (MWCNTs) or carbon nanofibers (CNFs) to polymeric melts offers a convenient route to obtain highly conductive plastics. However, when these materials are melt processed, their conductivity can be lost. Here, it is shown that conductivities can be recovered through melt annealing at temperatures above the polymer's glass transition temperature ($T_g$). We demonstrate these results for both MWCNT and CNF-based composites in polystyrene (PS). The mechanism behind the conductivity increase is elucidated through modeling. It involves a transition from aligned, unconnected particles prior to annealing to an interconnected network after annealing through viscoelastic relaxation of the polymer. Such re-arrangement is directly visualized for the case of the CNF-based composites using confocal microscopy. The annealing-induced increase in particle connectivity is also reflected in dynamic rheological measurements on both MWCNT and CNF composites as an increase in their elastic moduli at low frequencies.

© 2008 Elsevier Ltd. All rights reserved.

## 1. Introduction

Electrically conductive nano-particles, such as carbon nanotubes (MWCNTs) and carbon nanofibers (CNFs), have enjoyed immense attention over the last several years. These particles have been of great interest to polymer scientists because their inclusion into polymer matrices gives rise to conductive thermoplastics [1,2]. Indeed, the combination of high conductivity from the particles with the flexibility and easy processability of polymers is a highly desirable mixture. Materials with such unique properties are likely to enable new applications, such as lightweight radiation shields for use by NASA in outer space [3–5]. Accordingly, many groups have investigated polymer–MWCNT and polymer–CNF nanocomposites, and impressive conductivities have been reported. For example, conductivities around 1 S/m have been realized with loadings of just ca. 2 wt.% of MWCNTs [6,7] or 5 wt.% of CNFs [8].

The polymer–MWCNT/CNF composites studied previously have typically been prepared at a laboratory scale, often via solvent-processing or *in situ* polymerization techniques since these are amenable to small sample sizes [2,9–15]. One question for polymer scientists is whether the same materials can be produced on a much larger scale using conventional polymer processing techniques such as single-screw or twin-screw extrusion, compression or injection molding, or melt spinning. The present study arose out of our attempts to make polymer–MWCNT/CNF nanocomposites via twin-screw extrusion. To our surprise, the conductivities of extruded samples were disappointingly low. Indeed, an examination of the literature on this topic shows that a rather wide range of conductivity values have been reported, sometimes much lower than might be expected for a given particle loading [2,6,7,16,17]. These differences can be attributed generally to the range of processing methods and conditions used by different authors. It is clear that processing affects the conductivity and also other material properties. The question then is how can we maximize the conductivity of these materials and how can we recover the properties that might be lost after a processing step?

In this study, we show that a simple way to recover the electrical conductivities of polymer–MWCNT/CNF nanocomposites following processing is by melt annealing the materials at a temperature exceeding the glass transition temperature ($T_g$) of the polymer. The annealing step is shown to increase the room temperature conductivity by several orders of magnitude in some cases. Systematic effects on conductivity are observed as a function of annealing temperature and annealing time. Although similar

* Corresponding author.
** Corresponding author.
*E-mail addresses:* bruck@umd.edu (H.A. Bruck), sraghava@eng.umd.edu (S.R. Raghavan).

0032-3861/$ – see front matter © 2008 Elsevier Ltd. All rights reserved.
doi:10.1016/j.polymer.2008.08.057

observations have been mentioned in a couple of earlier studies [18,19] and have been reported in polymer–nanotube composite fibers [20], this is the first detailed study on annealing effects in bulk polymer–MWCNT/CNF nanocomposites to our knowledge. Our studies also explain why the conductivity is lost during processing in the first place, and why annealing increases it back. Specifically, the shear during processing is shown to align the MWCNT or CNF particles, which decreases their degree of interconnectivity and thereby the conductivity. When the material is annealed, however, the particle distribution becomes more isotropic and their connectivity thereby increases. The increase in connectivity due to annealing manifests also as an improvement in the elastic character of the nanocomposites, which we demonstrate through dynamic rheological experiments.

## 2. Experimental

### 2.1. Materials

Two polystyrene (PS)-based nanocomposites were investigated in this study. In one case, polystyrene was Styron 666D from Dow Chemical, with a weight-average molecular weight of 240,000 g/mol and a polydispersity index of 2.29. This was combined with multi-walled carbon nanotubes (MWCNTs) purchased from Hyperion Catalysis International as a masterbatch with a mass concentration of 20% in PS. The second system consisted of high-impact polystyrene (i.e., a PS with 5 wt.% copolymerized butadiene; weight-average molecular weight of 150,000 and polydispersity index of 2.73) obtained from Nova Chemicals, and this was combined with carbon nanofibers (CNFs) (PR-19 LHT from Pyrograf Products).

### 2.2. Nanocomposite sample preparation

For the PS/MWCNT, appropriate amounts of the PS and masterbatch pellets were fed into a twin-screw extruder (B & P Process Equipment; co-rotating, intermeshing, 25:1 *L*:*D*). The extruder was operated with a 400 rpm screw speed and a barrel temperature of 185 °C in all zones except the last zone, which was held at 195 °C. Samples with MWCNT mass concentrations of 1, 2, and 4% were prepared, with the extruded product being pellets (2 mm diameter, 5 mm length). For the PS/CNF, the PS pellets and the CNF were fed into a Werner–Pfleiderer twin-screw extruder (28 mm screw diameter, co-rotating, intermeshing, 30:1 *L*:*D*). A 60 rpm screw speed and a 210 °C barrel temperature were used for all zones except the last zone (165 °C). Samples with mass concentrations between 3 and 15% CNF were prepared as strips (25 mm width, 1 mm thickness).

For meaningful rheological and electrical conductivity measurements, it is necessary to have specimens of consistent sample geometry (size and shape) and normalized microstructure. The PS/CNF and PS/MWCNT composites were therefore compression molded in a Carver press using a circular die of diameter 25 mm and thickness 1 mm. The molding was done at a temperature of 150 °C for 10 min at a pressure of about 0.9 MPa. The reduction ratio used in the molding process was 0.67. This magnitude of reduction ratio is well known to produce significant shear deformation that promotes particle alignment.

The nanocomposites were melt annealed (henceforth referred to as annealed) at temperatures above the polymer's glass transition temperature ($T_g$). The choice of annealing temperature is crucial: it must be higher than the $T_g$ of PS ($\sim$100 °C), but below its thermal degradation temperature ($\sim$250 °C). We annealed at 170, 200, and 230 °C, each for 3 and 30 min. All annealing experiments were performed in a nitrogen atmosphere to avoid oxidative degradation of PS.

### 2.3. Conductivity measurements

The electrical conductivity of the composites was measured in accordance with ASTM D4496. Samples of a known cross-sectional area and thickness were placed between copper electrodes and the DC resistance was measured using a Fluke 87 multimeter. The surfaces of the sample in contact with the electrodes were coated with silver paint in order to reduce discrepancies arising from micro-roughness. It was ensured that the surface area of the electrodes exceeded the cross-sectional area of the discs.

### 2.4. Rheological measurements

Dynamic rheological experiments were performed on a RDAIII strain controlled rheometer (TA Instruments) equipped with a convection oven. A parallel plate geometry (25 mm diameter) was used with a gap of 0.9 mm. Frequency sweeps were obtained at 200 °C for the PS/MWCNT samples and at 170 °C for the PS/CNF samples; the choice of temperature being dictated by the thermal degradation temperature of the matrix polymer. Frequency spectra from 0.032 to 320 rad/s were obtained at a strain of 0.5%, which was verified to be in the linear viscoelastic regime of the sample. Before recording each frequency sweep, the sample was equilibrated at the test temperature usually for a period of 30 min; subsequent frequency sweeps after this time were reproducible within 0.5%. All rheological experiments were performed in a nitrogen atmosphere to avoid oxidative degradation of PS.

### 2.5. Confocal microscopy imaging

Direct analysis of particle distributions and alignment in the composite samples were evaluated at room temperature using a laser confocal microscope (Carl Zeiss Model LSM510). Confocal microscopy utilizes coherent laser light and collects reflected light exclusively from a single plane with a thickness of 100 nm (a pinhole sits conjugated to the focal plane and rejects light out of the focal plane). A red laser ($\lambda = 633$ nm) was used as the coherent light and images were taken with an Epiplan-Neofluar 100×/1.30 oil-pool objective. A filter (Rapp Optoelectronic LP385) was used to limit the lower spectra of reflected light. One hundred two-dimensional images (optical slices with 512 pixel × 512 pixel), with scan size 92.1 × 92.1 μm, were taken at a spacing of 100 nm by moving the focal plane in order to assess the three-dimensional morphology. Images were further analyzed using the NIH Image software program.

## 3. Results and discussion

### 3.1. Electrical conductivity

Fig. 1 presents the electrical conductivity $\sigma$ at room temperature of PS/MWCNT and PS/CNF nanocomposites before and after annealing. Consider the MWCNT results first (Fig. 1a). For the unannealed samples, the conductivities were too low to be detected over the entire range of MWCNT concentrations (the lower detection limit of our measurements is $10^{-8}$ S/m). We will show later that these surprisingly low values of $\sigma$ are due to the disruption of connectivity between the particles. The significant result from Fig. 1a is that the conductivity can be recovered by annealing. Annealing at 170 °C is seen to have a modest effect: $\sigma$ is increased for the 4% MWCNT sample but not for the others. On the other hand, annealing at 230 °C has a significant effect on $\sigma$ at all MWCNT concentrations: all the MWCNT samples are now conductive, and their $\sigma$ values approach ca. 1 S/m at the higher MWCNT concentrations. Note that, for the 4% MWCNT sample, the conductivity is raised by several orders of magnitude to about $10^{-2}$ S/m by

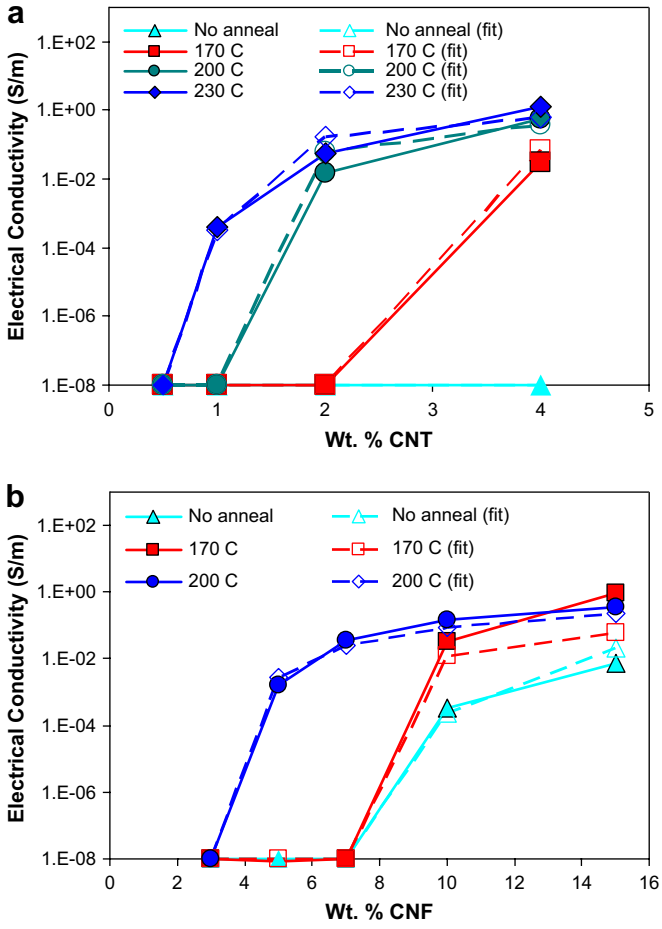


**Fig. 1.** Effect of annealing temperature on the conductivity of (a) PS/CNT and (b) PS/CNF nanocomposites. Samples were annealed for 30 min each. Note the significant increases in conductivity due to annealing. The conductivity of non-conductive samples is reported as $10^{-8}$ S/m since that is our lowest detection limit. Fits from a model of the time- and temperature-dependent electrical conductivity recovery behaviors can also be seen.

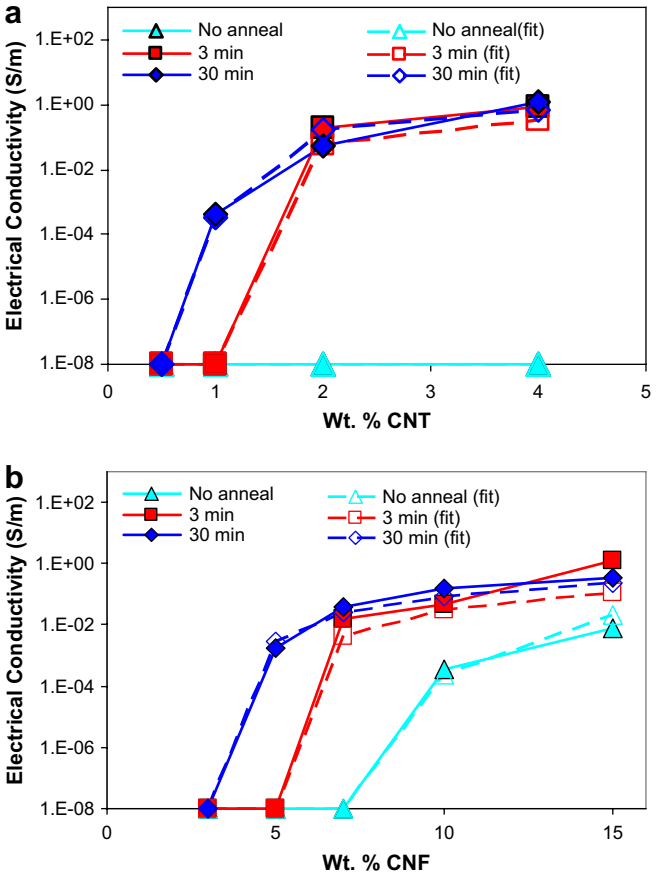


**Fig. 2.** Effect of annealing time on the conductivity of (a) PS/MWCNT nanocomposites annealed at 230 °C and (b) PS/CNF nanocomposites annealed at 200 °C. Fits from a model of the time- and temperature-dependent electrical conductivity recovery behaviors can also be seen.

annealing at 170 °C, and by two more orders of magnitude to ca. 1 S/m by annealing at 230 °C.

Similar trends in electrical conductivity can be observed for PS/CNF samples (Fig. 1b). Note that CNFs have a lower intrinsic conductivity as well as a lower aspect ratio than MWCNTs, and as a result, polymer/CNF composites have lower conductivities at a given particle loading compared to MWCNT-based systems [8]. Therefore, to obtain highly conductive polymer nanocomposites, one needs to use higher CNF loadings (note the higher values on the *x*-axis of Fig. 1b). The effects of annealing are very similar, however. In the absence of annealing, we could only detect appreciable conductivities for the 10 and 15% CNF samples. For these two samples, annealing at 170 °C for 30 min further enhances their conductivities by ca. two orders of magnitude. For the 5 and 7% CNF samples, annealing at 170 °C has a negligible effect, but annealing at 200 °C does impart significant conductivities.

Fig. 2 shows that in addition to annealing temperature, the annealing time also has an effect on the electrical conductivity of both PS/MWCNT (a) and PS/CNF (b) composites. For the PS/MWCNT samples, annealing time effects were investigated at 230 °C. The data in Fig. 2a show that the 4% PS/MWCNT sample attains the same conductivity whether it is annealed for 3 or 30 min at this temperature. On the other hand, the 2% MWCNT sample has a lower conductivity after a lower annealing time. The 1% sample remains an insulator if annealed for just 3 min, but becomes conductive after annealing for 30 min. Similarly, for the PS/CNF samples, annealing for a lower time of 3 min at 200 °C is sufficient for the 15% CNF sample, but at the lower CNF concentrations a longer annealing time of 30 min is necessary to fully restore the conductivity. Note that the error bars cannot be seen in Figs. 1 and 2 since they are smaller than the size of each data point.

### 3.2. Dynamic rheology

We will show that the above recovery of conductivity in MWCNT and CNF-based nanocomposites after annealing is due to the re-establishment of connections between the particles that were lost during processing. One way to establish the above link between properties and microstructure is to examine the dynamic rheology of samples before and after annealing. Dynamic rheology (measurements of the elastic modulus $G'$ and the viscous modulus $G''$ as functions of the frequency $\omega$) is a sensitive probe of the percolated network formed by particles in polymer nanocomposites. The presence of such a network manifests as a plateau in the elastic modulus $G'$ at low $\omega$, and the magnitude of this $G'$ plateau is known to correlate with the density of connections in the network.

Fig. 3 shows frequency sweeps at 200 °C for selected PS/MWCNT samples prior to and after annealing at 230 °C for 30 min. The results are especially notable for the 1% MWCNT sample (Fig. 3a). In this case, the unannealed sample does not show a low-$\omega$ plateau in its $G'$, which implies that there is no percolated MWCNT network in this sample. This observation helps to explain why this

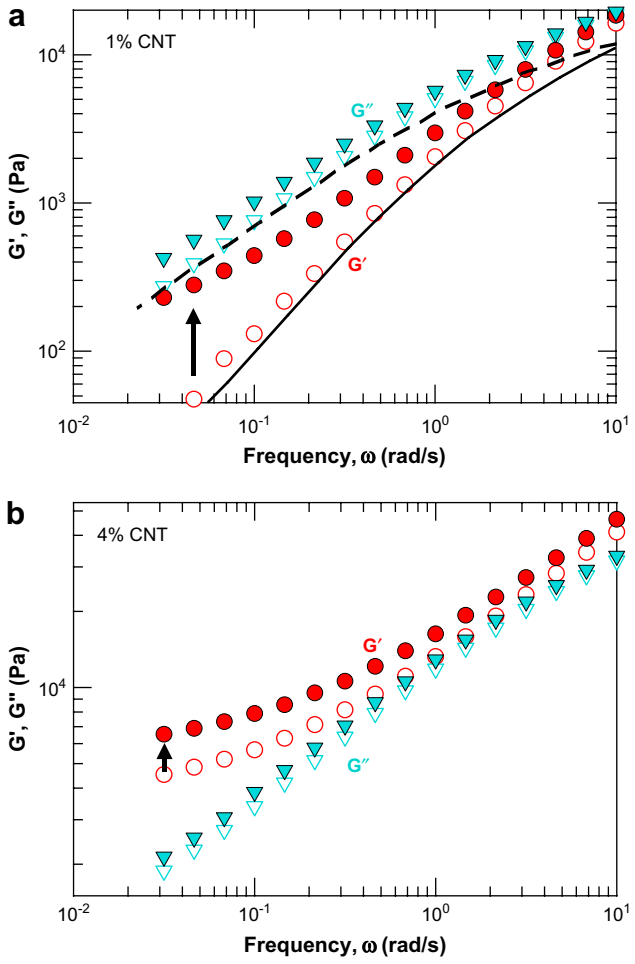


**Fig. 3.** Effect of annealing on the dynamic rheological properties at 200 °C of PS/MWCNT nanocomposites containing (a) 1 wt.% CNT and (b) 4 wt.% CNT. Data are shown for the elastic modulus $G'$ (circles) and the viscous modulus $G''$ (triangles) as functions of the frequency $\omega$ for an unannealed sample (open symbols) and a sample annealed at 230 °C for 30 min (filled symbols). In each case, $G'$ at low $\omega$ is increased by annealing, as shown by the arrows. For comparison the data for the pure PS are included, $G'$ (solid line) and $G''$ (dashed line).

unannealed sample showed negligible conductivity in Fig. 1a. On the other hand, upon annealing, the $G'$ plot levels off at low $\omega$, suggesting that a sample-spanning MWCNT network has been established. Comparing the two sets of data, at the lowest $\omega$, the value of $G'$ is increased by a factor of 5 due to annealing. Correspondingly, annealing also induces a small increase in the viscous modulus $G''$. Generally, network connectivity is primarily reflected in the elastic properties of the sample, which is why more significant changes are observed for $G'$ than $G''$. Similar increases in $G'$ at low $\omega$ are also found at other MWCNT concentrations and also for the CNF-based samples. For illustration, we also show data before and after annealing for the 4% MWCNT sample in Fig. 3b. In this case, there is already a $G'$ plateau at low $\omega$ for the unannealed sample, implying that a percolated MWCNT network does exist. Upon annealing, the $G'$ plateau increases in magnitude, indicating a higher density of network connections.

It should be noted that the rheological data in Fig. 3 are taken at 200 °C – the data then depict the structure of an annealed sample even prior to annealing at 230 °C. Thus, it is not a straightforward matter to compare annealed and unannealed samples using melt rheology. Indeed, it is then understandable that the differences in rheology at 200 °C are modest when compared to the differences in room temperature conductivities between the unannealed and annealed samples. Nevertheless, our rheological data are reproducible and consistent, i.e., the annealed sample is always the one that exhibits the higher moduli. Similar increases in low-frequency $G'$ are also seen for the PS/CNF composites. The rheological data are summarized in Fig. 4, which shows $G'/G''$ before and after annealing as a function of the MWCNT and CNF concentrations. The shifts in these results are consistent with a reduction in the percolation threshold [21] due to annealing (see Section 3.4).

### 3.3. Confocal microscopy

The dynamic rheological data are consistent with the hypothesis that interparticle connections are restored during annealing. To further substantiate this, we have directly visualized the structure in our composites using confocal microscopy. The MWCNTs used in our study were too small to be individually resolved by this technique (the pictures obtained were similar to those we have reported earlier [22]). However, the larger CNFs can be resolved quite nicely, and Fig. 5 shows typical micrographs of both unannealed (Fig. 4a) and annealed (b) PS/CNF samples at room temperature. The unannealed sample clearly shows substantial alignment of the CNFs. This is further illustrated in the Fourier transform of the micrograph for the unannealed sample, which shows an anisotropic pattern that is elongated normal to the alignment direction. Thus, it is clear that the CNF particles are significantly aligned, presumably due to the shear involved in the processing steps (i.e., extrusion, followed by compression molding). In contrast, the annealed sample (Fig. 4b) shows an

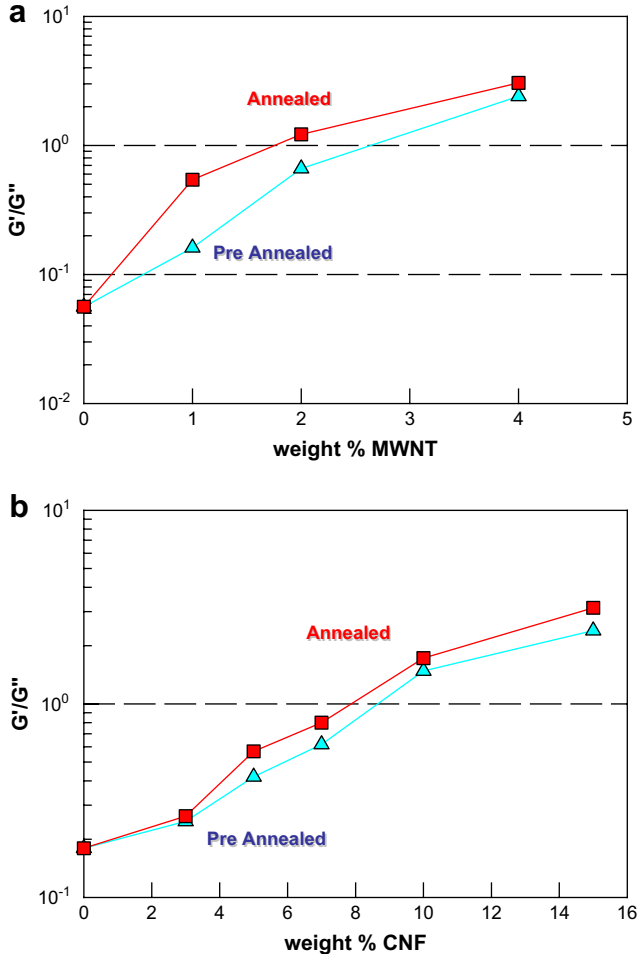


**Fig. 4.** Effect of annealing on nanocomposite firmness $G'/G''$ (a) PS/MWCNT annealed at $T = 230$ °C for 30 min and (b) PS/CNF annealed at $T = 230$ °C for 30 min.

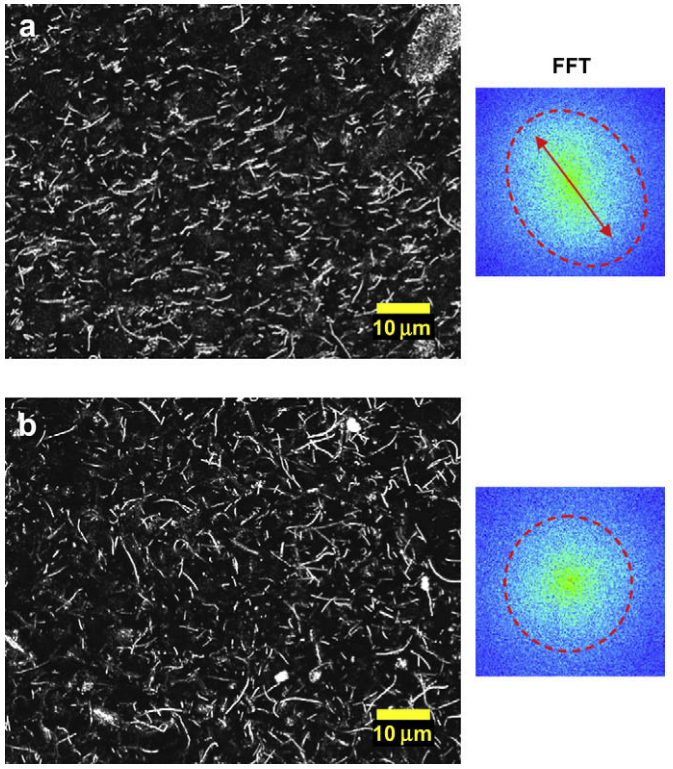


**Fig. 5.** Confocal microscopy images showing the effect of annealing on the microstructure of PS/CNF nanocomposites containing 3 wt.% CNF. (a) Unannealed sample, showing alignment of CNFs, as confirmed by the elongated Fourier transform of this image, shown on the right. (b) Annealed sample, showing a more isotropic orientation of the CNFs, as also seen from the isotropic shape of the Fourier transform image on the right.

isotropic distribution of the CNFs, and the Fourier transform of this image shows an isotropic pattern. Thus, the confocal images show that the action of annealing is to restore an isotropic distribution of particles, which, in turn, implies the re-establishment of connections in the particle network.

The idea that alignment implies a loss of particle interconnects, thereby delaying the onset of particle percolation in the matrix, has been advanced by others [23]. Similarly, other researchers have separately shown that particle alignment induced by high shear can adversely impact the dynamic rheological properties [12] and even the conductivity of polymer/MWCNT composites [10,11,17,24,25]. These studies, however, did not deal with the effects of annealing to restore the lost properties. To our knowledge, the impact of annealing on conductivity in polymer/MWCNT materials has only been considered in passing in a couple of papers [18,19], but has not been the focus of any study thus far. This is the first detailed investigation of annealing effects on MWCNT/CNF-based composites, especially in showing how changes in material properties are directly connected to changes in the microstructure.

### 3.4. Origin for annealing effects on particle distribution

It is worth considering how or why annealing is able to re-orient the aligned particles into an isotropic state. Nanocomposites are typically non-Brownian systems due to their high matrix viscosity and the extended geometry of the nano-particles [17,21,26,27]. Nevertheless, while translational and rotational diffusions may be limited, the particles may still be able to re-orient, even under non-Brownian conditions due to the viscoelastic nature of the polymer matrix. That is, the relaxation of polymer chains at the high annealing temperatures will facilitate the re-arrangement of the dispersed nano-particles (the higher the annealing temperature, the greater the particle re-orientation due to the decrease in polymer relaxation time, *cf.* Eq. (3) below). Also, note from our data (Figs. 1 and 2) that the nanocomposites with higher particle concentrations recover their conductivity after annealing at lower temperatures and for shorter times. This is because, at higher concentrations, the particles will be sufficiently close to each other that they can re-form interconnects quite easily. However, at lower concentrations, the particles will need to re-orient and/or translate appreciably to form a link with their nearest neighbors. Similar reorganization under quiescent conditions at high temperatures (after shear, for example) has been reported for clay particles in polymer/clay nanocomposites [26,27].

### 3.5. Modeling the conductivity increase due to annealing

To further understand the conductivity increase, we develop a model that relates the variation in conductivity to changes in connectivity between the MWCNTs/CNFs due to annealing. We start from the conventional power-law relationship used to describe the electrical conductivity $\sigma_c$ as a function of the particle volume fraction $\beta$.

$$\sigma_c(t,T) = \sigma_{PS} + A\{\beta(t,T) - \beta_C\}^{\lambda} \tag{1}$$

where $A$ is the power-law coefficient, $\lambda$ is the power-law exponent, $\beta$ is the volume fraction of interconnected particles, $\beta_C$ is the critical volume fraction for percolation, and $\sigma_{PS}$ is the conductivity of neat polystyrene. Note that we have modified this expression to reflect that both $\sigma_c$ and $\beta$ are dependent upon annealing time and temperature. Our key assumption in the light of Fig. 4 is that *particle alignment decreases the effective volume fraction of connected (percolated) particles*, which are the ones that contribute to the conductivity. In other words, the value of $\beta$ is initially less than that if the particle arrangement was completely isotropic, which we denote as $\beta_0$. The effect of annealing is to randomize the particle distribution, i.e., to increase $\beta$ until it approaches $\beta_0$. The variation of $\beta$ with annealing time $t$ and temperature $T$ is postulated to take on a stretched exponential relationship, as follows:

$$\beta = f\left(a - (a-1)e^{-(t/\tau(T))^p}\right) \tag{2}$$

where $\tau$ is a time constant that varies with temperature, $f$ is the total volume fraction of MWCNT or CNF reinforcement, $a$ is the fraction of reinforcement that is initially percolated, and $p$ is the stretching exponent. The key parameter here is the time constant $\tau$ for re-arrangement of the particles, and this can be considered proportional to the relaxation time of the viscoelastic polymer matrix. Thus, much like for a polymer well above its $T_g$, an Arrhenius relationship can be postulated for $\tau$ as follows:

$$\tau(T) = b\exp(E_a/RT) \tag{3}$$

where $b$ is the Arrhenius coefficient, $E_a$ the activation energy and $R$ the gas constant.

Fits of this model to the data are shown in Figs. 1 and 2 and the constants determined from the fits are summarized in Table 1. The constants we obtain are similar to those that we have reported previously for the percolation of polymer/MWCNT composites [9,21]. Note that the response of the CNFs to the viscoelastic relaxation of the polymer requires an $E_a$ of 3.14 kJ/mol, nearly 50% greater than for the MWCNTs. This implies that a longer annealing time (or a higher temperature) is required for full recovery of conductivity in the case of the CNFs. This result may not be unexpected since the CNFs are larger and rougher than the MWCNTs, substantially increasing their resistance to re-orientation. There is also a larger fraction of the CNFs that are percolated initially, with

**Table 1**
Constants determined from fitting a time- and temperature-dependent model to the data for electrical conductivity recovery due to melt annealing

| Constant | CNF | MWCNT |
|---|---|---|
| $\beta_c$ | 3 | 0.68 |
| $\sigma_{PS}$ | $10^{-8}$ S/m | $10^{-8}$ S/m |
| $A$ | 15 S/m | 70 S/m |
| $\lambda$ | 1.6 | 1.2 |
| $a$ | 0.31 | 0.11 |
| $p$ | −0.3 | −0.3 |
| $b$ | $1.7 \times 10^{23}$ | $1.8 \times 10^{15}$ |
| $E_a$ | 3.14 kJ/mol | 2.17 kJ/mol |

a value of 0.31 versus 0.11 for the MWCNTs. This would indicate that the CNFs are more resistant to alignment than the MWCNTs.

## 4. Conclusions

In this study, we have shown that the conductivities of PS/MWCNT and PS/CNF nanocomposites are decreased as a result of processing (by twin-screw extrusion and compression molding), but can be recovered by annealing at high temperatures. Similarly, the dynamic rheological properties, specifically the elastic modulus $G'$ at low frequencies, can also be increased by annealing. The microstructural basis for the above results is that, during processing, the particles become aligned in the flow direction, leading to a decrease in the connectivity of the particle network. The same connections, however, are re-established during annealing, which explains the recovery of the properties. Direct evidence for the above mechanism has been obtained by confocal microscopy. We believe that our results may have practical relevance for the large-scale manufacture of conductive polymer nanocomposites.

## Acknowledgements

BHC and SRR gratefully acknowledge funding from the NIST BFRL extramural grants program through grant no. 70NANB4H1001. AKK and HAB acknowledge support by ONR award number N000140710391. Helpful discussions with Prof. Robert Briber of the Materials department at UMD are also acknowledged.

## References

[1] Baughman RH, Zakhidov AA, de Heer WA. Science 2002;297:787–92.
[2] Moniruzzaman M, Winey KI. Macromolecules 2006;39:5194–205.
[3] Dalton AB, Collins S, Munoz E, Razal JM, Ebron VH, Ferraris JP, et al. Nature 2003;423:703.
[4] Ramasubramaniam R, Chen J, Liu HY. Appl Phys Lett 2003;83:2928–30.
[5] Smith JG, Connell JW, Delozier DM, Lillehei PT, Watson KA, Lin Y, et al. Polymer 2004;45:825–36.
[6] Potschke P, Abdel-Goad M, Alig I, Dudkin S, Lellinger D. Polymer 2004;45:8863–70.
[7] Potschke P, Dudkin SM, Alig I. Polymer 2003;44:5023–30.
[8] Lozano K, Bonilla-Rios J, Barrera EV. J Appl Polym Sci 2001;80:1162–72.
[9] Kota AK, Cipriano BH, Duesterberg MK, Gershon AL, Powell D, Raghavan SR, et al. Macromolecules 2007;40:7400–6.
[10] Dalmas F, Chazeau L, Gauthier C, Masenelli-Varlot K, Dendievel R, Cavaille JY, et al. J Polym Sci Part B Polym Phys 2005;43:1186–97.
[11] Du FM, Scogna RC, Zhou W, Brand S, Fischer JE, Winey KI. Macromolecules 2004;37:9048–55.
[12] Du FM, Fischer JE, Winey KI. Phys Rev B 2005;72.
[13] Gojny FH, Wichmann MHG, Fiedler B, Kinloch IA, Bauhofer W, Windle AH, et al. Polymer 2006;47:2036–45.
[14] Sandler JKW, Kirk JE, Kinloch IA, Shaffer MSP, Windle AH. Polymer 2003;44:5893–9.
[15] Stephan C, Nguyen TP, Lahr B, Blau W, Lefrant S, Chauvet O. J Mater Res 2002;17:396–400.
[16] McNally T, Potschke P, Halley P, Murphy M, Martin D, Bell SEJ, et al. Polymer 2005;46:8222–32.
[17] Kharchenko SB, Douglas JF, Obrzut J, Grulke EA, Migler KB. Nat Mater 2004;3:564–8.
[18] Alig I, Lellinger D, Dudkin SM, Potschke P. Polymer 2007;48:1020–9.
[19] Xu YJ, Higgins B, Brittain WJ. Polymer 2005;46:799–810.
[20] Miaudet P, Bartholome C, Derré A, Maugey M, Sigaud G, Zakri C, et al. Polymer 2007;48:4068–74.
[21] Kota A, Cipriano BH, Powell D, Raghavan S, Bruck HA. Nanotechnology 2007;18:505705.
[22] Cipiriano BH, Kashiwagi T, Raghavan SR, Yang Y, Grulke EA, Yamamoto K, et al. Polymer 2007;48:6086–96.
[23] Bicerano J, Douglas JF, Brune DA. J Macromol Sci Rev Macromol Chem Phys 1999;C39:561–642.
[24] Potschke P, Brunig H, Janke A, Fischer D, Jehnichen D. Polymer 2005;46:10355–63.
[25] Obrzut J, Douglas JF, Kharchenko SB, Migler KB. Phys Rev B 2007;76:195420.
[26] Ren JX, Casanueva BF, Mitchell CA, Krishnamoorti R. Macromolecules 2003;36:4188–94.
[27] Solomon MJ, Almusallam AS, Seefeldt KF, Somwangthanaroj A, Varadan P. Macromolecules 2001;34:1864–72.